Chitosan/siRNA Nanoparticles Encapsulated in PLGA Nanofibers for siRNA Delivery

Menglin Chen,[†,*] Shan Gao,[†,‡] Mingdong Dong,[†] Jie Song,[†] Chuanxu Yang,[†,‡] Kenneth Alan Howard,[†,‡] Jørgen Kjems,[†,‡] and Flemming Besenbacher[†,§]

[†]Interdisciplinary Nanoscience Center (iNANO), [‡]Department of Molecular Biology and Genetics, and [§]Department of Physics and Astronomy (IFA), Aarhus University, DK-8000 Aarhus C, Denmark

ABSTRACT

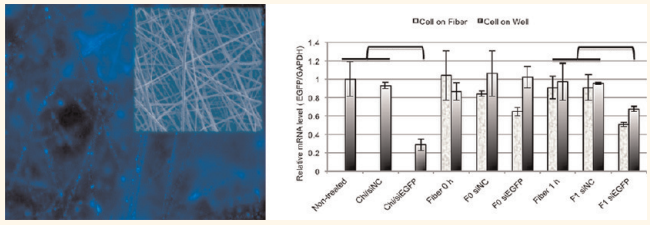

Composite nanofibers of biodegradable poly(D,L-lactic-*co*-glycolic acid) (PLGA) encapsulating chitosan/siRNA nanoparticles (NPs) were prepared by electrospinning. Acidic/alkaline hydrolysis and a bulk/surface degradation mechanism were investigated in order to achieve an optimized release profile for prolonged and efficient gene silencing. Thermo-controlled AFM *in situ* imaging not only revealed the integrity of the encapsulated chitosan/siRNA polyplex but also shed light on the decreasing T_g of PLGA on the fiber surfaces during release. A triphasic release profile based on bulk erosion was obtained at pH 7.4, while a triphasic release profile involving both surface erosion and bulk erosion was obtained at pH 5.5. A short alkaline pretreatment provided a homogeneous hydrolysis and consequently a nearly zero-order release profile. The interesting release profile was further investigated for siRNA transfection, where the encapsulated chitosan/siRNA NPs exhibited up to 50% EGFP gene silencing activity after 48 h post-transfection on H1299 cells.

KEYWORDS: nanofibers · chitosan · siRNA · electrospinning · release · gene silencing

The concept of controlling the release of therapeutically active agents using polymers is an established approach that has been used in the clinic.[1,2] Encapsulation of medicinal drugs increases drug efficacy, specificity, tolerability, and therapeutic index of corresponding drugs.[3] Understanding the release mechanism is an important requirement to design an optimal release system. The active agents can be dispersed within the polymer matrix or a core encapsulated by a polymeric diffusional barrier. A desirable zero-order drug delivery system is one in which the active agents are fully immobilized within a biodegradable matrix where diffusion is of little consequence and bioerosion is confined to the outer surface.

Thermoplastic aliphatic polyesters such as poly(D,L-lactic-*co*-glycolic acid) (PLGA) have been widely used for controlled release devices due to excellent biocompatibility and biodegradability.[4] The polyester PLGA undergoes hydrolytic degradation to form the two monomers, lactide (L) and glycolide (G), which then enter the tricarboxylic acid cycle and are easily metabolized.

Electrospinning is a simple, but versatile process that produces continuous nanoscale fibers through the action of an external electric field imposed on a rich variety of materials that include synthetic or natural polymers, inorganic or organic compounds, and blends. Combining its nano features with the ability of incorporating electronic, magnetic, optical, or biological functionalities, it has seen rapid development that holds great promise in tissue engineering, drug delivery, electronic and optical nanodevices, *etc.*[5−9] Not surprisingly, the induced resemblance of natural extracellular matrix (ECM) nanostructure could intrinsically contribute to the synergy of contact guidance and biochemical signals to mediate and support cellular development in regenerative medicine.[10,11]

RNA interference (RNAi)[12] is a promising strategy to interrupt gene expression. RNAi involves double-stranded small interfering RNA (siRNA) molecules 21−22 nucleotides in length that mediate sequence-specific enzymatic cleavage of target mRNA through complementary base pairing. This allows specific suppression of gene expression[13] as a tool for investigating cellular gene functions and as a therapeutic drug. The therapeutic potential of siRNA, however, is restricted by its susceptibility

* Address correspondence to menglin@inano.au.dk.

Received for review January 9, 2012 and accepted May 23, 2012.

Published online May 23, 2012
10.1021/nn300106t

to serum degradation, renal clearance, and poor cellular uptake due to its polyanionic nature. Nanoparticles have been developed to improve pharmacokinetics, cellular delivery, and intracellular trafficking of siRNA.[14] Nanoparticles formed by the electrostatic self-assembly of siRNA with the polysaccaride chitosan are a promising system to improve the efficiency of gene silencing.[15−18]

siRNA release through electrospun nanofibers[19,20] has been demonstrated successfully using poly(caprolactone) (PCL) and poly(ethylene glycol) (PEG) mixtures,[20] or copolymer of PCL and ethyl ethylene phosphate (EEP),[19] with or without MirusTKO as a transfection agent during siRNA encapsulation in nanofibers. The mechanism of the release, however, has not been fully investigated. It is suggested that the release is based on diffusion, while a higher burst release is related to enhanced hydrophilicity of the polymer matrix by either mixing PEG[20] or copolymerizing with EEP.[19]

In this work we describe the first study to elucidate the release mechanism of a delivery system combining chitosan/siRNA NPs and PLGA nanofibers produced by simple co-electrospinning. The release mechanism based on acidic or alkaline hydrolysis of PLGA was investigated using a release study combining scanning electron microscopy (SEM) and atomic force microscopy (AFM). The integrity of chitosan/siRNA NPs was studied using gel electrophoresis, and its bioactivity was investigated by enhanced green fluorescent protein (EGFP) knockdown experiments on H1299 cells.

RESULTS AND DISCUSSION

Encapsulation of Chitosan/siRNA Nanoparticles (NPs) in PLGA Nanofibers. Chitosan/siRNA polyplex formation relies on the electrostatic interaction between the ammonium cations in chitosan and phosphate anions in siRNA; therefore, the stability and net charge of the polyplex are highly affected by the pH values of the solution.[21] The pK_a values of phosphates are near 0; therefore, more than 99% of phosphates are negatively charged when the pH is above 2. The pK_a of ammonium cations in chitosan is 6.5; therefore, theoretically ~91% of amines are protonated and positively charged at pH 5.5. Thus, the preformed interpolyelectrolyte complexes at pH 5.5 using N/P 10 are highly positively charged and facilitate cellular uptake. However, when they are released to biological conditions at pH 7.4, theoretically only 11.2% of amines remain protonated. Therefore N/P 10 was chosen in order to have a relative excess of ammonium cations than phosphate anions at pH 7.4 to allow maximum loading of siRNA.

Uniform composite fibers with 0.26 w/w % NPs containing Cy5-labeled siRNA at 350−400 ng/mg concentration were produced by electrospinning. SEM and fluorescence imaging shows that the NPs were effectively encapsulated in electrospun fibers with a diameter of 864 ± 350 nm (Figure 1). No surface enrichment of the NPs was observed, which is consistent with XPS analysis (Figure S1) showing surfaces consisting of PLGA-derived carbon and oxygen. The derived [N]/[C] ratio from the wide energy survey scans is 3:2, close to the theoretical value of 11:8 from PLGA (L:G = 3:1).

Although the blend solutions of PLGA and chitosan/siRNA NPs in miscible hexafluoro-2-isopropanol (HFIP)/H_2O is homogeneous before electrospinning, the possible phase separation during electrospinning has previously been demonstrated.[22] Drawing of the nanofibers with high surface area leads to a rapid solvent evaporation rate at a time scale down to the millisecond range during the electrospinning process. The rapid evaporation of solvents not only generally increases the concentration of the solution, which leads to solidification, but also in our system specifically induces incompatibility of PLGA and chitosan/siRNA NPs; due to the higher boiling point of water (100 °C) compared to HFIP (58.2 °C), the ratio of HFIP to water in the solution will decrease during evaporation. Considering the large difference of solubility of chitosan/siRNA NPs and PLGA in water, the viscosity of PLGA increases more rapidly than that of the polyplex aqueous droplets; therefore phase separation is thermodynamically favored. Kinetically, these differences provide PLGA with high mobility to overcome the viscous friction of the mixture to complete the coalescence process of phase separation prior to solidification. The rapid elongation and stretching of the nanofibers also destabilize the colloidal system, causing an inward movement of aqueous droplets. Consequently, PLGA formed a skin layer at the surface.

PLGA Degradation. The hydrophilic chitosan/siRNA NPs were released during degradation of PLGA. In order to elucidate the release mechanism of chitosan NPs, it is very important to understand the hydrolytic degradation of PLGA.

Water uptake initially occurs when PLGA samples are immersed in an aqueous environment. As the number and size of water-filled pores in the polymer increase, a porous connected network, allowing hydrophilic drug release, is formed.

Hydrolysis of PLGA is generally catalyzed by weak acids (a reversible reaction generating carboxylic acids and alcohols) or by alkalines (a nonreversible reaction generating carboxylates and alcohols).

Hydrolytic degradation in physiological medium results from two critical phenomena. First, degradation causes an increase in the number of carboxylic terminal chains, which are known to autocatalyze ester hydrolysis. Second, only oligomers soluble in the surrounding aqueous medium can escape from the matrix. Over time, soluble oligomers that are close to the surface can leach out before full degradation, whereas those that are located well within the matrix remain

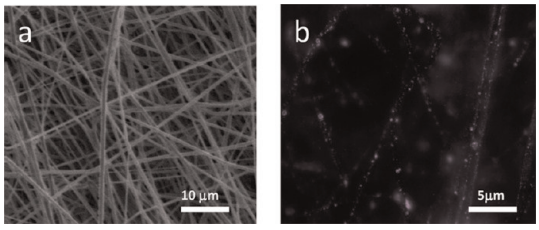

Figure 1. SEM (a) and fluorescence (b) images of the chitosan/siRNA-Cy5 NP-encapsulated PLGA fibers.

entrapped and contribute totally to the autocatalytic effect. The local autocatalytic phenomenon is known to cause heterogeneous degradation inside, more rapid at the center than at the surface.[23] The resulting difference in concentration of acidic groups leads to the formation of a tube composed of less degraded polymer. Therefore, it is possible that a significant part of the total transport resistance occurs at the surface; consequently, PLGA undergoes bulk erosion instead of surface erosion.

Kinetics of hydrolysis depends on many factors that affect molecular mobility and accessibility of polymers to water: (1) the composition of PLGA monomers: the more lactide present, the more hydrophobic polymer chains appear and eventually the slower the hydrolysis becomes;[4] (2) the molecular weight and T_g: the lower M_w and T_g are, the more mobile polymeric chains become, leading to faster hydrolysis; (3) morphology of the materials: more surface area creates more reactive sites exposed to facilitate the hydrolysis. However, those factors vary continuously during the hydrolysis and influence each other, which increases the complexity and lowers the predictability of the system. Since T_g decreases when M_w decreases, the increased mobility of chains can lead to both pore connection and closure due to polymer chain relaxation and rearrangement.

Degradation under Physiological Conditions (pH 7.4). Morphological changes of the fibers upon autocatalyzed degradation in 0.01 M phosphate buffer at pH 7.4 were monitored by SEM during the release study. The fibers became swollen and welded after 10 days of degradation. After 20 days, complicated pore closure and connection were observed. After 50 days the fibrous morphology was totally lost, and the samples became brittle and crystalline (Figure 2).

In an attempt to shed further light on the surface morphology, atomic force microscopy studies allowing imaging at the nanoscale were thus performed with the fibers after a release study at pH 7.4 for 20 days. All the maps are presented as bright images based on quantitative values of measurable physical properties; the brighter the pixel is, the higher the values are. The topographies (Figure 3a, d), which can be directly related to the actual surface morphologies, are not sufficient to identify the surface composition. The variations in stiffness (Figure 3b, e) and adhesion force (Figure 3c, f) in different areas provide complementary insight into the local surface physical and chemical properties. Evidently, at 20 °C the PLGA molecules run perpendicular to the fiber axis interrupted with chitosan/siRNA NPs, which corresponds to the relatively more adhesive and stiffer areas, considering the polarity of the NPs and the crystalline chitosan with $T_g \approx 204$ °C[24] (Figure 3a–c). This demonstrated the successful integration of the NPs in the fibers, which again proved that interpolyelectrolyte systems can survive the electrospinning process.[25]

Furthermore, an *in situ* temperature-controlled AFM study demonstrated that when the temperature was raised to 37 °C (Figure 3d–f), movement of the NPs along with PLGA started on the surface, which can be observed by the changes of both the texture of the PLGA molecules and the positions of the NPs. In general PLGA has a T_g ranging from 40 to 60 °C depending on the G/L ratio and the M_w.[26] During degradation, polymer M_w decreased and molecular mobility became greater, leading to decreased T_g. Therefore, this interesting phenomenon proved that while polymer chains shortened upon degradation at pH 7.4 for 20 days, the T_g of short PLGA (or oligo LGA) at the surface had decreased to around 37 °C.

Degradation under Slightly Acidic Conditions. The degradation in 0.01 M sodium acetate buffer at pH 5.5 introduced similar morphology changes: the fibers became swollen and welded, and the fibrous morphology was gradually lost. Faster degradation was found, suggesting both surface erosion and bulk erosion were involved with the aid of acidic catalysis (Figure S2).

Degradation under Slightly Alkaline Conditions. On the other hand, hydrolysis under alkaline conditions is generally rapid and nonreversible due to the synergy of alkaline catalysis and the hydrophilic carboxylate products, which encourage water contact. Simultaneoulsy, the device undergoes surface erosion resulting from the fast hydrolysis with a negative gradient of diffussing OH^- ions from the surface to the center. The degradation of the PLGA fibers containing chitosan/siRNA NPs under alkaline conditions in 10 μM NaOH showed typical features of surface erosion. SEM images (Figure 4) showed that fiber diameter decreased while the alkaline pretreatment time increased. On the other hand, an increasing number of NPs were exposed on the nanofiber surfaces.

siRNA Release Study and Proposed Mechanism. The cumulative release profiles of siRNA release was monitored for 50 days *in vitro* under three different buffer or pretreatment conditions (Figure 5): (1) under neutral conditions in 0.01 M phosphate buffer (pH 7.4), (2) under slightly acidic conditions in 0.01 M sodium acetate buffer (pH 5.5), and (3) under 0.01 M phosphate buffer (pH 7.4) after pretreating fibers for 1 h in the presence of 10 μM NaOH.

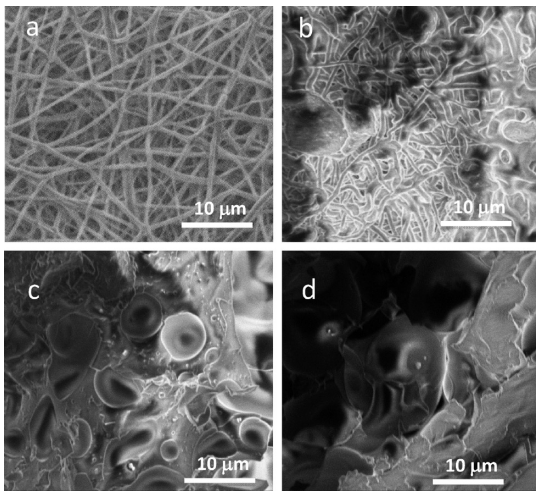

Figure 2. SEM images of the fibers after release study at pH 7.4 for 0 day (a), 10 days (b), 20 days (c), and 50 days (d).

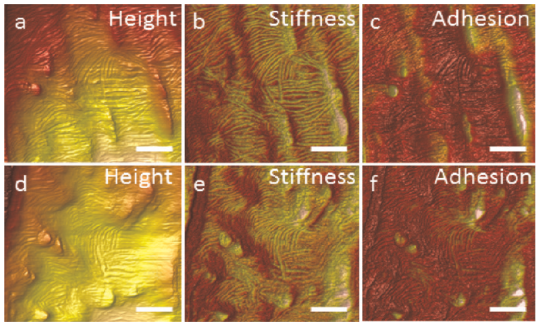

Figure 3. *In situ* temperature-controlled AFM images (scale bar 200 nm) of the fibers after a 20-day release study at pH 7.4: (a–c) 20 °C; (d–f) 37 °C.

Release under pH Neutral Conditions. To investigate the release under physiological conditions while exploring the interesting autocatalytic nature of PLGA degradation under physiological conditions, a release study was conducted at pH 7.4.

When the fibers were incubated under neutral conditions (pH 7.4 in 0.01 M phosphate buffer), a triphasic profile was obtained; a low initial burst followed by a sustained zero-order release and then a fast second burst around day 20. According to the degradation study, the initial burst is related to the diffusion of the chitosan/siRNA NPs close to the surface, while the rest of the release is dependent on the degradation. Considering the dominating autocatalysis phenomenon, it is likely that a skin layer of polymer was formed by slower degradation. In this case a second burst is often seen as corresponding to the crack of the skin layer. On the other hand, AFM analysis (Figure 3) shows at day 20 the surface PLGA T_g decreased to around physiological temperature, 37 °C, indicating that the increased PLGA mobility could be a synergic effect on accelerating the release, corresponding to the second burst.

Release under Weak Acidic Conditions. Under acidic conditions, although H^+ ions catalyze the hydrolysis,

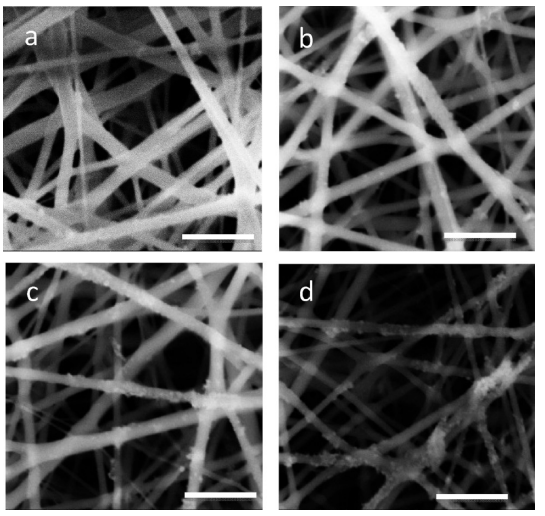

Figure 4. SEM images of the fibers (scale bar 5 μm) after 10 μM NaOH pretreatment for 0.5 h (a), 1 h (b), 5 h (c), and 12 h (d).

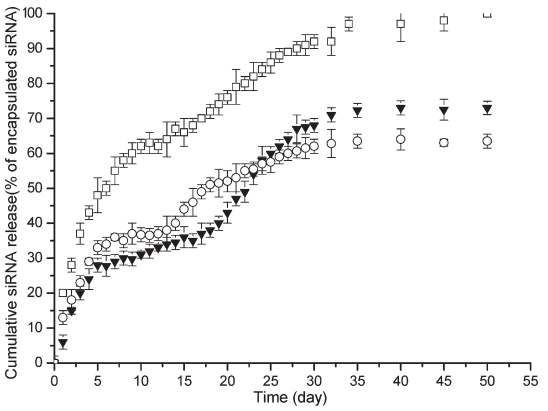

Figure 5. Release profile of siRNA in buffer solution containg (1) 0.01 M phosphate buffer (pH 7.4) (filled triangles), (2) 0.01 M sodium acetate buffer (pH 5.5) (empty circles), and (3) 0.01 M phosphate buffer (pH 7.4) after treating the fibers 1 h in the presence of 10 μM NaOH (empty squares).

earlier studies[27] demonstrated a lower degradation rate at pH ≤4 compared to at pH 7.4, probably due to the reversibility of the reaction and the generation of hydrophobic carboxylic acids (pK_a ~5, ≥91% protonation), which repel water and kinetically slow the reaction. Here we monitored a release based on acidic hydrolysis using a medium solution of pH 5.5, where theoretically 76% carboxylic acid would be deprotonated and hydrophilic, while 90% of chitosan amines remained protonated for forming a positive interpolyelectrolyte complex with siRNA.

Compared to the release at pH 7.4, a similar triphasic profile was obtained at pH 5.5: faster initial burst followed by a shorter zero-order release and then a slower second burst with a, however, lower overall release. Faster initial burst could be related to the acidic catalysis surface degradation. The second burst again proved the complexity of acidic hydrolysis, which is consistent with the degradation study, where both

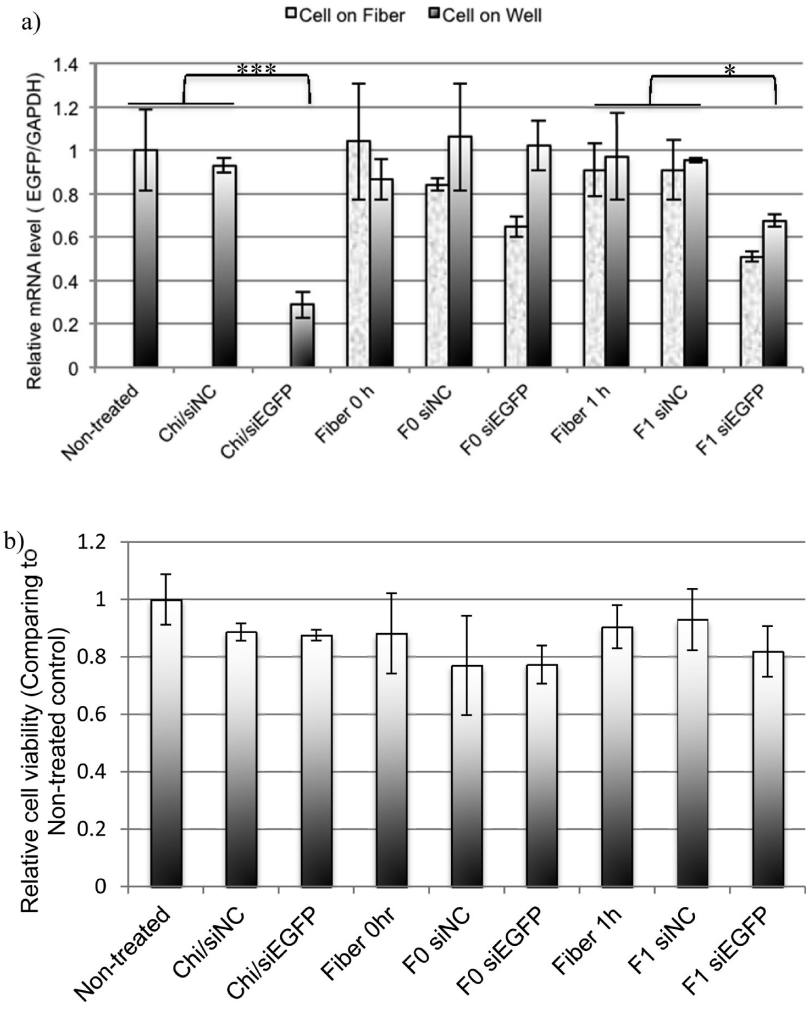

Figure 6. (a) Silencing of EGFP gene expression in H1299 cells using nanofibers encapsulating chitosan/siEGFP NPs; (b) cell viability of transfected H1299 cells. (a) After 48 h transfection with siEGFP or negative control siNC, cells from both the well bottom and the nanofiber surface were harvested separately. Total RNA was isolated, and real-time PCR was performed. EGFP mRNA expression levels were normalized against the level of internal control, GAPDH. Data were obtained from three independent experiments and presented as mean ± SD ($n = 3$). The knockdown effect was compared with the expression level of nontreated cells (set to 1). ***, $p < 0.001$ and *, $p < 0.05$ evaluated by Student's t test, respectively. (b) MTT assay was performed at 48 h post-transfection. The relative absorbance (A570) was measured and normalized to the level of the nontreated control. Data were obtained from three independent experiments and presented as mean ± SD ($n = 3$). Nontreated: H1299 cells without transfection; Chi/siEGFP: cells transfected with chitosan/siEGFP nanoparticles; Chi/siNC: cells transfected with chitosan/siNC (negative control siRNA from Genepharm, Shanghai) nanoparticles; Fiber 0 h and Fiber 1 h: PLGA fiber without and with 1 h alkaline pretreatment, respectively; F0 siNC and F1 siNC: cells transfected *via* nanofibers encapsulated with chitosan/siNC without and with 1 h alkaline pretreatment, respectively; F0 siEGFP and F1 siEGFP: cells transfected *via* nanofibers encapsulated with siEGFP without and with 1 h alkaline pretreatment, respectively.

surface erosion and bulk erosion were found. The lower overall release of chitosan/siRNA NPs is probably due to the electrostatic forces between the carboxylate degradation product and the NPs.

Release under Physiological Conditions Assisted by Short Alkaline Catalysis. Although hydrolysis at alkaline conditions is generally favorable, considering hydrolysis of RNA might occur when pH ≥ 9, a short pretreatment of 10 μM NaOH for 1 h was conducted. Interestingly, a near zero-order release profile was observed. The release profile suggests a nearly homogeneous degradation was obtained after the alkaline pretreatment, which may open up the skin PLGA layer and increase the pore size through the fiber. This could prevent autocatalysts building up inside and consequently simplify the release process.

siRNA Integrity and Bioactivity. *siRNA integrity.* Northern analysis was used to assess the integrity of siRNA released from the electrospun fibers. As shown in Figure S3, siRNA was found essentially intact even from samples collected at 8, 29, and 50 days.[17,21]

While the short alkaline pretreated nanofiber demonstrated the ideal, nearly zero-order release profile, the alkaline effect on siRNA integrity and bioactivity of chitosan-mediated siRNA delivery is still unknown. To investigate the influence of alkaline treatment on the siRNA integrity, siRNA was extracted from extended alkaline-pretreated nanofibers, varing from 0.5 to 12 h.

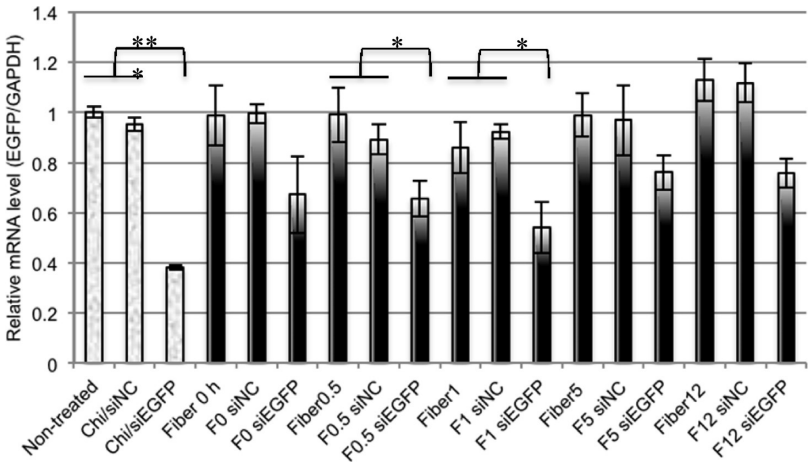

Figure 7. Evaluation of gene silence efficacy *via* the siEGFP containing fibers with extended alkaline pretreatment. Nontreated, Chi/siNC, and Chi/siEGFP were set up as described in Figure 6; F0.5 siEGFP, F1 siEGFP, F5 siEGFP, and F12 siEGFP represent cells transfected *via* siEGFP containing fibers pretreated with alkaline for 0.5, 1, 5, and 12 h, respectively. Following the same procedures of pretreatment with alkaline, pure PLGA fibers and fibers formulated with chi/siNC were included for each time point as controls and represented as Fiber0.5 to Fiber12 and F0.5 siNC to F12 siNC, respectively. ***, $p < 0.001$ and *, $p < 0.05$ evaluated by Student's *t* test.

Intact siRNA was found for all the samples on a 6% denaturing polyacrylamide gel, suggesting an interesting protective milieu for siRNA from degradation that the nanofibers might provide.

Furthermore, a native 2% agarose gel for the same samples demonstrated a retardation of the samples compared to the naked siRNA, matching the migration of the chitosan/siRNA NP control, indicating that associated chitosan/siRNA NPs are present after the alkaline treatment (Figure S4). As mentioned, the stability and net charge of the chitosan/siRNA polyplex is highly affected by the pH values of the solution. Considering there was less than 1% of amines in chitosan remaining protonated during the short alkaline pretreatment, dissociation of chitosan/siRNA NPs (N/P = 10) would most likely occur. However, as chitosan is soluble in water only when a certain amount of amines are protonated, precipitation of chitosan together with the siRNA may occur before their dissociation, as seen in the SEM image in Figure 4.

Efficacy of Gene Silencing. The bioactivity of chitosan/siRNA NPs after being encapsulated in the composite fibers was investigated in a 48 h siRNA transfection on H1299 cells. The release study illustrated that the most interesting release profile was obtained using a weak alkaline pretreatment. Accordingly, compared to the chitosan/siEGFP NPs encapsulated fibers without alkaline treatment, higher EGFP gene silencing (~50%) was obtained when the composite fibers were pretreated under alkaline conditions for 1 h, with statistical significance compared with nontreated control, pure PLGA fiber, and fiber-chitosan/siNC ($p < 0.05$ evaluated by Student's *t* test), respectively (Figure 6a). Considering the positive knockdown that was observed, in combination with the integrity study (Figure S4), it is thus presumed that upon weak alkaline treatment, the siRNA remained intact in its polyplex form with chitosan, which can be released into the medium at pH 7.4 as positive charged NPs ready for cellular uptake.

EGFP expression level was downregulated in both cells from the well bottom and cells on the nanofibers. The gene silencing effect on cells seeded on the nanofibers was generally higher than that of the cells on the well bottom. This is consistent with earlier studies,[19,20] where nanofibers assisting the transfection of siRNA yielded enhanced knockdown. This suggests a synergy of topographic induction of the nanofibers with the bioactivities: the fibrous morphology assisted local siRNA uptake or cell susceptibility to RNA interference.

Cell Viability. The cell viability in the nanofiber-mediated transfection is under the synergistic influence of the cytotoxicity caused by the transfection reagent and the surface chemistry of the nanofibers.[19,20] To investigate the cell viability on the chitosan/siEGFP NP-encapsulated fibers, an MTT assay was performed at 48 h post-transfection with pure PLGA fibers or NP-encapsulated fibers (Figure 6b). Compared to the nontreated control, the viability of cells cultured with pure nontreated PLGA fibers was ~90%, which was similar to the toxicity level observed for cells transfected with chitosan/siRNA NPs alone. The viability of cells cultured on chitosan/siRNA NP-encapsulated fibers was ~80%, demonstrating the cumulative effect of both the fibrous carrier and the NP exposure. The alkaline hydrolytic pretreatment turned the hydrophobic surface moderately hydrophilic, consequently favoring cell adhesion.[28] Accordingly, the cell viability increased about 5−15%.

Effects of Alkaline Pretreatment Time on siRNA Transfection Efficacy. Furthermore, in order to investigate the impact of extended pretreating times on siRNA

transfection efficacy, the fibers were pretreated with the weak alkaline varing from 0.5 to 12 h before cell seeding and fiber-mediated transfection. Both pure PLGA fiber and fibers formulated with chitosan/siNC controls were included for each time point. As seen in Figure 7, both pretreatments for 1 and 0.5 h resulted in significant down-regulation of EGFP level compared with either pure PLGA fibers or fibers containing NC control siRNA (fiber-chi/siNC control) ($p < 0.05$), while the fibers with the extended alkaline pretreatment for 5 and 12 h demonstrated less EGFP knockdown, with no statistically significant difference compared with nontreated controls ($p > 0.05$). Quantification of the siRNA that was extracted out from the 5 and 12 h alkaline-treated fibers showed only a 5−10% diffusional loss of siRNA during the prolonged alkaline pretreatment. Therefore, the lower silencing efficiency from the prolonged alkaline treatment is still unclear, which is probably due to a lower release of chitosan/siRNA NPs related to stronger electrostatic forces between the larger amount of carboxylate product from alkaline hydrolysis and the NPs.

Furthermore, a maintained silencing of EGFP was observed using 1 h alkaline-treated fibers at day 10 (Figure S5), where in general gene knockdown from a single transfection directly using chitosan/siRNA NPs will not last more than a week, and stable gene silencing is observed only up to 3 days.[29] This indicates that the chitosan NPs with structurally intact siRNA with retained bioactivity were continuously released from the fibers and conducted repeated transfection on the cells. Hence, a simple pretreatment using 10 μM NaOH for 1 h was found optimal for EGFP silencing, demonstrating that the short, weak alkaline pretreatment can increase the skin PLGA layer porosity with minimum disturbance to the encapsulated bioactives.

CONCLUSIONS

We have presented the first and interesting release mechanism study of chitosan/siRNA NPs from electrospun PLGA nanofibers. Composite fibers with siRNA dosages of 350−400 ng/mg PLGA were produced by electrospinning. The formation of a PLGA skin layer during electrospinning is suggested with both thermodynamic/kinetic factors and field-driven effects considered.

The release mechanism based on PLGA degradation was thoroughly investigated considering both acidic and alkaline hydrolysis, where the pH values were carefully chosen considering both PLGA hydrolysis kinetics and the challenge of chitosan/siRNA polyplex stability in the system. Thermo-controlled AFM *in situ* imaging not only revealed the integrity of the encapsulated chitosan/siRNA polyplex but also shed light on the decreasing T_g of PLGA on the fiber surfaces during release, correlating to the second burst release. A triphasic release profile based on PLGA bulk erosion was obtained at pH 7.4; a triphasic release profile involving both surface erosion and bulk erosion of PLGA was obtained at pH 5.5, while a short alkaline pretreatment provided a more homogeneous PLGA hydrolysis and a nearly zero-order release profile.

Although siRNA is suspected under alkaline hydrolysis, the integrity study demonstrated nearly essentially intact siRNA, suggesting PLGA nanofibers serve as a protective milieu for siRNA from hydrolysis. The bioactivity of chitosan/siRNA NPs was found to be retained and prolonged after being encapsulated in the composite nanofibers; especially those with short alkaline pretreatment exhibited up to 50% silencing efficacy upon 48 h transfection with prolonged activity up to 10-days duration. Therefore, the short, weak alkaline pretreatment can increase the skin PLGA layer porosity with minimum disturbance to the encapsulated bioactives, which leads to a nearly ideal, zero-order long-term release profile.

Furthermore, the gene silencing effect was more pronounced for cells seeded on the nanofibers than those situated in the well, indicating a synergy of topographic induction of the ECM mimic nanofibers with the bioactivities: the fibrous morphology assisted cell adhesion and local siRNA uptake.

This study again indicates electrospinning is an extremely attractive nanomedicine fabrication method due to its simplicity, robustness, and versatility. We believe the combination of simple alkaline pretreatment and straightforward electrospinning technique could ensure the utility of PLGA nanofibers as drug carriers for many other different types of drugs.

EXPERIMENTAL SECTION

Materials. PLGA lactide:glycolide (75:25), M_w = 66 000−107 000, and hexafluoro-2-isopropanol (HFIP) were purchased from Sigma Aldrich. Chitosan (250 kDa, 100% deacetylation) was produced by Bioneer A/S (Hbrsholm, Denmark). EGFP-specific siRNA duplex was purchased from Ribotask, Odense, Denmark, containing the sequences sense, 5′-GACGUAAACG-GCCACAAGUUC-3′, and antisense, 5′-ACUUGUGGCCGUUUAC-GUCGCU-3′, and the control siRNA duplex was chosen as a negative control siRNA (siNC), provided by Genepharm, Shanghai, China, containing the sequences sense, 5′-UUCUCCGAAC-GUGUCACGUTT-3′, and antisense, 5′-ACGUGACACGUUCGGAG-AATT-3′, both used for electrospinning and EGFP interference work. siEGFP containing a fluorescent Cy5-labeled 5′ sense strand was used for fluorescence imaging and release experiment.

Preparation of Chitosan/siRNA NPs. The interpolyelectrolyte complexes between siRNA duplexes (21-mers) and chitosan (N:P = 10:1) were prepared as reported.[30] Chitosan was dissolved in sodium acetate buffer (0.3 M sodium acetate, pH 5.5) to obtain a 1 mg/mL solution. A 360 μL sample of the 1 mg/mL

chitosan solution was added to 140 μL of sodium acetate buffer (300 mM, pH = 5.5). During stirring, 60 μL (N:P = 10:1) of siRNA (100 μM siEGFP or siNC) was added and left for 1 h.

Electrospinning. PLGA (85 mg) was added to 0.25 mL of HFIP and stirred for 2 h. Then 0.25 mL of the freshly made chitosan/siRNA NPs (siEGFP and siNC) in pH 5.5 acetate buffer was added, and the solution was stirred for another 0.5 h. The homogeneous solutions were placed in a 1 mL syringe fitted with a metallic needle of 0.6 mm inner diameter. The syringe was fixed horizontally on the syringe pump (model KDS101, KD Scientific), and an electrode of high-voltage power supply (Spellman High Voltage Electronics Corporation, MP Series) was clamped to the metal needle tip. The flow rate of polymer solution was 1 mL/h, and the applied voltage was 18 kV. The tip-to-collector distance was set to 12 cm, and a grounded stationary rectangular metal collector (15 cm $\times$ 20 cm) covered by a piece of clean aluminum foil was used for the fiber collection. Pure PLGA fibers from 17 w/v % solution in HFIP were also prepared.

Measurements and Characterization. The fiber morphology was examined by high-resolution scanning electron microscopy (FEI, Nova 600 NanoSEM) at 5 kV. The fibers were placed directly into the SEM chamber without any metal sputtering or coating.

X-ray photoelectron spectroscopy (XPS) was performed using a Kratos Axis Ultra^{DLD} instrument equipped with a monochromated Al Kα X-ray source ($h\nu$ = 1486.6 eV) operating at 15 kV and 15 mA (225 W). The fiber samples that were analyzed were cut from the Al foil containing a thick layer of fibers. A hybrid lens mode was employed during analysis (electrostatic and magnetic), with an analysis area of approximately 300 μm $\times$ 700 μm. For each sample, a takeoff angle of 0° (with respect to the sample surface) was used, allowing a maximum probe depth (10 nm). Wide energy survey scans were obtained over the range 0−1200 eV binding energy (BE) at a pass energy of 160 eV and used to determine the surface elemental composition.

Fluorescence imaging was conducted using a Zeiss Axiovert 200 M epifluorescence microscope (Carl Zeiss GmgH, Jena, Germany) equipped with Zeiss Filterset 10.

AFM-Based Nanomechanical Mapping. AFM-based quantitative nanomechanical mapping was performed by Multimode SPM (Nanoscope V controller, Veeco Instruments). The samples were placed on a commercially available controlled heating stage. The cantilever was maintained at the same temperature as the sample to maintain better imaging stabilities at each temperature. The cantilever is a HarmoniX probe (HMX-10) purchased from Bruker AFM Company. The cantilever for nanoscale material property mapping of standard samples is in the 10 MPa to 15 GPa hardness range. The spring constant is 17 N/m. (The parameters: Geometry is anisotropic, tip height is 4−10 μm, tip radius is 10 nm.) We imaged samples as in Figure 3 in tapping-mode AFM with harmonic torsion mode under ambient conditions. The effective elastic modulus was derived from these waveforms using our previously described mathematical procedure. The interactions between the tip and sample were determined by the long-range electrostatic and van der Waals forces, and short-range mechanical restoration forces. The topography, elastic modulus, and adhesion maps were processed using SPIP software (Image Metrology ApS, Lyngby, Denmark).

Release Study. A 5 mg amount of fibrous mesh was suspended in 1.0 mL of 0.01 M sodium acetate buffer (pH 5.5) or 0.01 M phosphate buffer (pH 7.4) in a 1.5 mL plastic vial (n = 3), in order to study the release under weak acidic conditions and physiological conditions. Then the suspension was placed in a shaking bath at 40 rpm and 37 °C for 50 days. At preset intervals, 0.2 mL of the supernatant was drawn and replaced by the fresh buffer accordingly.

The third release profile was obtained using short alkaline-treated fibers: 5 mg of fibrous mesh was treated with 10 μM NaOH for 1 h, followed by two PBS washings. The solutions were collected in order to check the diffusional loss of siRNA during the alkaline pretreatment and wash, where no siRNA was found. Then samples were suspended in 0.01 M phosphate buffer (pH 7.4) for the release study as described above.

All the samples after the 50-day release study were dissolved in 1 mL of chloroform followed by extraction with 200 μL of DEPC-treated TE buffer, in order to determine the siRNA remaining inside the fibers.

The siRNA in the supernatants and extracted out after the release studies was determined by a Ribogreen RNA quantitive kit and quantified by a Victor X5Multilabel plate reader (PerkinElmer).

siRNA Integrity Study. *siRNA Precipitation and Purification.* During the release study from nontreated fibers at pH 7.4, three supernatants from day 8, 29, and 50 were concentrated in a freeze dryer for 24 h. To samples with a volume of around 40−50 μL were added 1 μL of glycogen (Roche Diagnostics, Indianapolis, IN, USA), 0.1 volume of 3 M sodium acetate (pH = 6), and 2.5 volumes of 96% ethanol, and the solution was mixed thoroughly. The mixtures were left on dry ice for 20 min and centrifuged at full speed for 30 min. The supernatant was removed, and the white pellet was washed by 75% ethanol four times until the salt was washed out. The RNA pellet was dissolved in 20 μL of RNase-free water.

For alkaline-pretreated fibers, we extracted siRNA by dissolving 0.5 mg of fibers in 1 mL of chloroform followed by extraction with 200 μL of DEPC-treated TE buffer.

Gel Electropheresis and Northern Blotting. The RNA was run on 15% denaturing polyacrylamide gels, and 0.1 ng of naked siEGFP was loaded as control. The gel was transferred onto a Hybond-N$^+$ membrane (Amersham Biosciences). After UV cross-linking, the membranes were probed with [γ-^{32}P] ATP-labeled sense strand LNA modified siRNA according to standard procedures of Northern blotting.[31]

To investigate the RNA integrity for the alkaline-pretreated samples, the extracted RNA was run on 6% denaturing polyacrylamide gels in 1 $\times$ SB buffer (NaOH 10 mM, boric acid 28 mM, pH = 8.0), 15W/45 min. To investigate the NP association for the alkaline-pretreated samples, the samples were run on 2% agarose in 1 $\times$ SB buffer, 12W/30 min. Gel was stained by SYBR Green and visualized by a Typhoon scanner. To compare the efficiency of extraction from the fibers, the siRNA duplex, chitosan/siRNA NPs and the size ladder were included as controls for both gels. The loading amount of siRNA and chitosan/siRNA NPs was equal to 50 ng of siRNA

RNA Interference in EGFP-Expressing Human Cell Lines. *Cell Lines and Transfection.* Nanoparticle-mediated knockdown of endogenous EGFP was assessed in H1299 human lung carcinoma cell lines. This cell line, produced to express EGFP stably (EGFP half-life 2 h), was a gift from Dr. Anne Chauchereau (CNRS, Villejuif, France).

In order to compare the gene silencing efficacy with or without alkaline pretreatment, 9 groups (n = 3) were set up and were either not transfected (nontreated control and pure PLGA fibers) or transfected either directly by chitosan/siRNA NPs or *via* chitosan/siRNA-encapasulated fibers with or without 1 h pretreatment in 10 μM NaOH.

In order to evaluate the effect of extended alkaline pretreatment, cells were transfected *via* fibers encapsulated with siEGFP with 0.5, 1, 5, and 12 h alkaline pretreatment, respectively. The solutions after alkaline pretreatment and washing were collected in order to check the diffusional loss of the siRNA during the process.

For nontreated control and cells transfected directly by chitosan/siRNA NPs (siEGFP or siNC), cells were plated on multiwell 24-well plates (10^5 cells/well) in 100 μL of complete medium (containing 10% fetal bovine serum, 1% gentamysin) 3 h prior to transfection. For transfection, 400 μL of complete medium was added together with 3 μL of the prepared chitosan/siRNA (EGFP siRNA as positive control or NC siRNA as negative control) NPs, to match the loading of siRNA in 1.0 mg fibers with the final concentration at 64 nM.

Transfection through the fiber samples was conducted by seeding cells (10^5 cells/well) in 100 μL of complete medium on the fibers, which were prewetted with PBS pH 7.4 and placed on the bottom of the multiwell 24-well plates. Then 400 μL of complete medium was added after 3 h. The medium was totally changed for all the samples after 20 h with 500 μL of fresh complete medium.

The cells were harvested at 48 h post-transfection for qPCR analysis. For 10 days post-transfection, cells on the fibers with

1 h alkaline treatment were further incubated for 8 days and monitored by fluorescene microscopy.

Fluorescence Microscopy. Fluorescence microscopy (Olympus TH4-200) was used to monitor the suppression of EGFP for living cells before they were harvested. The downregulated EGFP expression could be observed according to fluoresecent signal intensity and the numbers of EGFP expressing cells.

Quantitative Real-Time RT PCR (qPCR). Some cells migrated on the bottom of the well from the fibers; we therefore lysed the cells from the well and cells on the fibers separately. Total RNA was isolated using TRIzol reagent following the procedures recommended by the manufacturer (Invitrogen, Copenhagen). Reverse transcription was carried out using the SuperScript II Reverse Transcriptase (RT) kit according to the manufacturer's protocol (Invitrogen, Copenhagen). Quantitative real-time RT PCR was performed as described previously[32] on a Mx4000 Multiplex Quantitative PCR System (Stratagene, Copenhagen). The comparative CT (threshold cycle) method described in the manufacturer's protocol was used to quantitate the relative EGFP mRNA expression level, comparing treated samples to concordant nontreated controls. The glyceraldehydes 3-phosphate dehydrogenase (GAPDH) gene mRNA was amplified as an internal control to normalize the data of the EGFP mRNA level. The primer sequences for the *EGFP* gene are as follows: forward 5′-AGAACGGCATCAAGGTGAAC-3′, reverse 5′- TGCTCAGGTAGTGGTTGTCG-3′, with a product size of 135 bp. Primer sequences for GAPDH gene are as follows: forward 5′-GGTCGGAGTCAACGGATTT-3′ and reverse 5′-CCAGCATCGCCCCACTTGA-3′, with a product size of 258 bp.[32]

Cell Viability Assay. The viability of transfected cells was determined by the MTT assay. Cells were plated in a 48-well plate for transfection. H1229 cells were seeded at densities of 5×10^4 cells/well, and the same transfection procedure was implemented with proportionally reduced amounts of siRNA and transfection reagent ($n = 3$). MTT reagent (5 mg/mL, Sigma, Copenhagen) was then added to each well at 1:3 dilution at 48 h post-transfection, after exchanging the medium. After incubating ~0.5 to 1 h at 37 °C, the reaction was stopped by replacing the DMSO while the color changes became visible. The relative absorbance (A570) was measured using a Victor X5Multilabel plate reader (PerkinElmer).

Statistical Analyses. Statistical significance was determined by the paried Student's *t* test, to assess the significant differences of the gene silencing effect between nanofiber-mediated transfection and controls.

Conflict of Interest: The authors declare no competing financial interest.

Acknowledgment. We gratefully acknowledge the Danish Council for Strategic Research for the funding to the Project "Electrospun Biomimetic Nanofibres as Regenerative Medicines (ElectroMed)" at the iNANO Center, the Lundbeck Foundation for support through the grant Lundbech Foundation Nanomedicine Center for Individualized Management of Tissue Damage and Regeneration (LUNA), and the Carlsberg Foundation for financial support.

Supporting Information Available: XPS and SEM spectra for the chitosan/siRNA NP-encapsulated PLGA fibers. Gel electrophoresis characterization for the integrity of chitosan/siRNA NPs. SEM and fluorescence images of H1299 cells on the chitosan/siRNA NP-encapsulated PLGA fibers. This material is available free of charge *via* the Internet at http://pubs.acs.org.

REFERENCES AND NOTES

1. Jeong, S. Y.; Kim, S. W. Biodegradable Polymeric Drug Delivery Systems. *Arch. Pharm. Res.* **1986**, *9*, 63–73.
2. Venkataraman, S.; Hedrick, J. L.; Ong, Z. Y.; Yang, C.; Ee, P. L. R.; Hammond, P. T.; Yang, Y. Y. The Effects of Polymeric Nanostructure Shape on Drug Delivery. *Adv. Drug Delivery Rev.* **2011**, *63*, 1228–1246.
3. Kumari, A.; Yadav, S. K.; Yadav, S. C. Biodegradable Polymeric Nanoparticles Based Drug Delivery Systems. *Colloids Surf. B Biointerfaces* **2010**, *75*, 1–18.
4. Fredenberg, S.; Wahlgren, M.; Reslow, M.; Axelsson, A. The Mechanisms of Drug Release in Poly(lactic-co-glycolic acid)-based Drug Delivery Systems—a Review. *Int. J. Pharm.* **2011**, *415*, 34–52.
5. Lu, X.; Wang, C.; Wei, Y. One-Dimensional Composite Nanomaterials: Synthesis by Electrospinning and Their Applications. *Small* **2009**, *5*, 2349–2370.
6. Agarwal, S.; Wendorff, J. H.; Greiner, A. Progress in the Field of Electrospinning for Tissue Engineering Applications. *Adv. Mater.* **2009**, *21*, 3343–3351.
7. Chen, M.; Besenbacher, F. Light-Driven Wettability Changes on a Photoresponsive Electronspun Mat. *ACS Nano* **2011**, *5*, 1549–1555.
8. Song, J.; Kahveci, D.; Chen, M. L.; Guo, Z.; Xie, E. Q.; Xu, X. B.; Besenbacher, F.; Dong, M. D. Enhanced Catalytic Activity of Lipase Encapsulated in PCL Nanofibers. *Langmuir* **2012**, *28*, 6157–6162.
9. Song, J.; Chen, M. L.; Olesen, M. B.; Wang, C. X.; Havelund, R.; Li, Q.; Xie, E. Q.; Yang, R.; Boggild, P.; Wang, C.; *et al.* Direct Electrospinning of Ag/Polyvinylpyrrolidone Nanocables. *Nanoscale* **2011**, *3*, 4966–4971.
10. Yoo, H. S.; Kim, T. G.; Park, T. G. Surface-Functionalized Electrospun Nanofibers for Tissue Engineering and Drug Delivery. *Adv. Drug Delivery Rev.* **2009**, *61*, 1033.
11. Sill, T. J.; von Recum, H. A. Electrospinning: Applications in Drug Delivery and Tissue Engineering. *Biomaterials* **2008**, *29*, 1989–2006.
12. Fire, A.; Xu, S.; Montgomery, M. K.; Kostas, S. A.; Driver, S. E.; Mello, C. C. Potent and Specific Genetic Interference by Double-Stranded RNA in *Caenorhabditis elegans*. *Nature* **1998**, *391*, 806–811.
13. Elbashir, S. M.; Harborth, J.; Lendeckel, W.; Yalcin, A.; Weber, K.; Tuschl, T. Duplexes of 21-Nucleotide RNAs Mediate RNA Interference in Cultured Mammalian Cells. *Nature* **2001**, *411*, 494–498.
14. de Wolf, H. K.; Snel, C. J.; Verbaan, F. J.; Schiffelers, R. M.; Hennink, W. E.; Storm, G. Effect of Cationic Carriers on the Pharmacokinetics and Tumor Localization of Nucleic Acids after Intravenous Administration. *Int. J. Pharm.* **2007**, *331*, 167–175.
15. Mao, S.; Sun, W.; Kissel, T. Chitosan-Based Formulations for Delivery of DNA and siRNA. *Adv. Drug Delivery Rev.* **2010**, *62*, 12–27.
16. Liu, X.; Howard, K. A.; Dong, M.; Andersen, M. O.; Rahbek, U. L.; Johnsen, M. G.; Hansen, O. C.; Besenbacher, F.; Kjems, J. The Influence of Polymeric Properties on Chitosan/siRNA Nanoparticle Formulation and Gene Silencing. *Biomaterials* **2007**, *28*, 1280–1288.
17. Howard, K. A.; Rahbek, U. L.; Liu, X.; Damgaard, C. K.; Glud, S. Z.; Andersen, M. O.; Hovgaard, M. B.; Schmitz, A.; Nyengaard, J. R.; Besenbacher, F.; *et al.* RNA Interference *in Vitro* and *in Vivo* Using a Novel Chitosan/siRNA Nanoparticle System. *Mol. Ther.* **2006**, *14*, 476–484.
18. Mittnacht, U.; Hartmann, H.; Hein, S.; Oliveira, H.; Dong, M.; Pego, A. P.; Kjems, J.; Howard, K. A.; Schlosshauer, B. Chitosan/siRNA Nanoparticles Biofunctionalize Nerve Implants and Enable Neurite Outgrowth. *Nano Lett.* **2010**, *10*, 3933–3939.
19. Rujitanaroj, P. O.; Wang, Y. C.; Wang, J.; Chew, S. Y. Nanofiber-Mediated Controlled Release of siRNA Complexes for Long Term Gene-Silencing Applications. *Biomaterials* **2011**, *32*, 5915–5923.
20. Cao, H.; Jiang, X.; Chai, C.; Chew, S. Y. RNA Interference by Nanofiber-Based siRNA Delivery System. *J. Controlled Release* **2010**, *144*, 203–212.
21. Katas, H.; Alpar, H. O. Development and Characterisation of Chitosan Nanoparticles for siRNA Delivery. *J. Controlled Release* **2006**, *115*, 216–225.
22. Chen, M.; Dong, M.; Havelund, R.; Regina, V. R.; Meyer, R. L.; Besenbacher, F.; Kingshott, P. Thermo-Responsive Core-Sheath Electrospun Nanofibers from Poly(N-isopropylacrylamide)/Polycaprolactone Blends. *Chem. Mater.* **2010**, *22*, 4214–4221.
23. Ding, A. G.; Schwendeman, S. P. Acidic Microclimate pH Distribution in PLGA Microspheres Monitored by Confocal

Laser Scanning Microscopy. *Pharm. Res.* **2008**, *25*, 2041–2052.
24. Dong, Y. M.; Ruan, Y. H.; Wang, H. W.; Zhao, Y. G.; Bi, D. X. Studies on Glass Transition Temperature of Chitosan with Four Techniques. *J. Appl. Polym. Sci.* **2004**, *93*, 1553–1558.
25. Yang, Y.; Li, X.; Cheng, L.; He, S.; Zou, J.; Chen, F.; Zhang, Z. Core-Sheath Structured Fibers with pDNA Polyplex Loadings for the Optimal Release Profile and Transfection Efficiency as Potential Tissue Engineering Scaffolds. *Acta Biomater.* **2011**, *7*, 2533–2543.
26. Middleton, J. C.; Tipton, A. J. Synthetic Biodegradable Polymers as Orthopedic Devices. *Biomaterials* **2000**, *21*, 2335–2346.
27. Liu, W. H.; Song, J. L.; Liu, K.; Chu, D. F.; Li, Y. X. Preparation and *in Vitro* and *in Vivo* Release Studies of Huperzine A Loaded Microspheres for the Treatment of Alzheimer's Disease. *J. Controlled Release* **2005**, *107*, 417–427.
28. Vanwachem, P. B.; Beugeling, T.; Feijen, J.; Bantjes, A.; Detmers, J. P.; Vanaken, W. G. Interaction of Cultured Human-Endothelial Cells with Polymeric Surfaces of Different Wettabilities. *Biomaterials* **1985**, *6*, 403–408.
29. Malmo, J.; Sorgard, H.; Varum, K. M.; Strand, S. P. siRNA Delivery with Chitosan Nanoparticles: Molecular Properties Favoring Efficient Gene Silencing. *J. Controlled Release* **2012**, *158*, 261–268.
30. Andersen, M. O.; Howard, K. A.; Kjems, J. RNAi Using a Chitosan/siRNA Nanoparticle System: *in Vitro* and *in Vivo* Applications. *Methods Mol. Biol.* **2009**, *555*, 77–86.
31. Gao, S.; Dagnaes-Hansen, F.; Nielsen, E. J.; Wengel, J.; Besenbacher, F.; Howard, K. A.; Kjems, J. The Effect of Chemical Modification and Nanoparticle Formulation on Stability and Biodistribution of siRNA in Mice. *Mol. Ther.* **2009**, *17*, 1225–1233.
32. Gao, S.; Skeldal, S.; Krogdahl, A.; Sorensen, J. A.; Andreasen, P. A. CpG Methylation of the PAI-1 Gene 5′-Flanking Region is Inversely Correlated with PAI-1 mRNA Levels in Human Cell Lines. *Thromb. Haemostasis* **2005**, *94*, 651–660.